Chinese Chemical Letters 36 (2025) 110165

Contents lists available at ScienceDirect

Chinese Chemical Letters

journal homepage: www.elsevier.com/locate/cclet

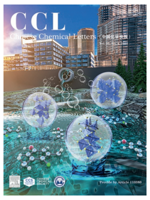

Organometallic modification of silica with europium endowing the fluorescence properties: The key technique for numerical quality monitoring

Junqing Wu[a], Yiyang Zhang[a,b,*], Qingqing Hong[c], Hui Yang[d], Lifeng Zhang[e], Ming Zhang[a], Lei Yu[a,*]

[a] School of Chemistry and Chemical Engineering, Yangzhou University, Yangzhou 225002, China
[b] School of Mechanical Engineering, Yangzhou University, Yangzhou 225127, China
[c] College of Information Engineering, Yangzhou University, Yangzhou 225127, China
[d] College of Environmental Science and Engineering, Yangzhou University, Yangzhou 225127, China
[e] Department of Electrical and Electronic Engineering, Kyushu Institute of Technology, Kitakyushu, Fukuoka 8048550, Japan

ARTICLE INFO

Article history:
Received 28 February 2024
Revised 12 June 2024
Accepted 21 June 2024
Available online 22 June 2024

Keywords:
Fluorescence
Silica
Fillers
Hybrid material
Composites

ABSTRACT

The micro-dispersion structure of silica fillers exerts significant influences on the performance characteristics of rubber-based products. How to monitor this parameter is an important issue in the rubber industry, but there is currently no suitable technical solution for numerical monitoring that can be applied in automatic production line. The labeling of silica in rubber is a challenge that bottlenecks the development of numerical quality monitoring technology. In this work, we employed the organometallic europium to modify silica endowing the fluorescence properties for characterization. It provides more feasible solutions for visually studying the relationship between the submicroscopic structure and macroscopic properties of inorganic-filled polymers, and is the key foundation for achieving numerical monitoring of rubber filler qualities in industry.

Silica is one of the most crucial reinforcing fillers in rubber products, as it effectively enhances the mechanical properties of the materials and reduces the product costs [1,2]. However, the hydroxyl groups on silica particle surfaces make it prone to agglomeration during the industrial processing, resulting in the stress concentration that compromises the final product quality [3]. Analyzing the microscopic data of silica dispersion allows for the provision of theoretical support in studying the mechanism of action of fillers in rubber and establishing a connection between macroscopic properties and microscopic dispersion [4]. LSCM may provide an efficient method for analyzing the status of the fillers. In comparison with the conventional analysis techniques such as scanning electron microscopy (SEM), transmission electron microscopy (TEM), atomic force microscopy (AFM), and synchrotron X-ray nano-computed tomography [5-15], LSCM has the advantages of easy operation, low sample damage, and high cost-effectiveness, and has been widely used in the biomedical field [16-21]. Therefore, after further numerical transformation of the signals, it is possible to apply the technique in automatic product quality monitoring in industrial production [22-24]. However, due to the lack of fluorescence in silica itself, it cannot provide any signal feedback in LSCM analysis [25-29]. Thus, molecular modification of silica is required to endow the material high fluorescence quantum yield, long fluorescence lifetime, and good resistant to fluorescence quenching, so that the clear image data can be obtained [30-36]. Recently, we developed a novel method for modifying silica by introducing the organometallic europium into the material and resolved the bottlenecked issue in this industry. Herein, we wish to report our findings.

As shown in Scheme 1, aminopropyltriethoxysilane (APTES) was initially employed to modify silica *via* the transesterification reaction on the orthosilicic acid site in APTES. The prepared intermediate APTES/SiO_2 contained amine and could easily react with phthalic anhydride (PhA) *via* amide formation to produce PhA-Si/SiO_2, the material bearing a free carboxylic acid group. Rare metals can usually form strong coordination bonds with carboxylic acids [37]. Consequently, refluxing PhA-Si/SiO_2 with europium salt and 1,10-phenanthroline (phen) ligand in EtOH yielded the organometallic europium-modified silica Eu(PhA-Si)$_3$phen/SiO_2.

---

[*] Corresponding authors.
E-mail addresses: 008011@yzu.edu.cn (Y. Zhang), yulei@yzu.edu.cn (L. Yu).

https://doi.org/10.1016/j.cclet.2024.110165
1001-8417/

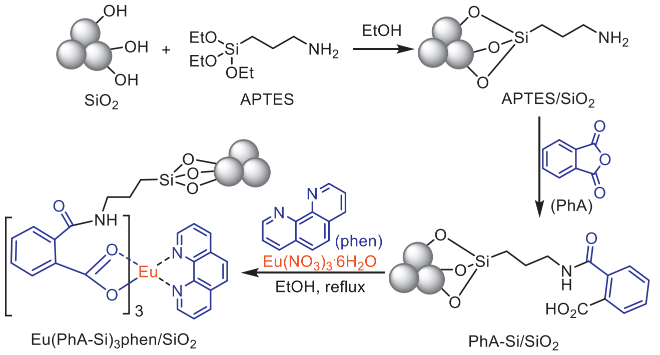

Scheme 1. Diagram of the synthetic route of fluorescent modification silica.

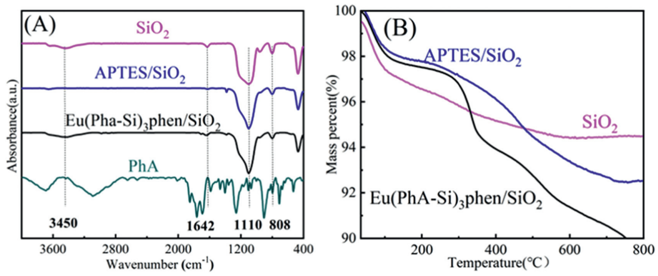

Fig. 1. Characterizations of the materials. (A) FT-IR spectra of silica (SiO$_2$), APTES/SiO$_2$, Eu(PhA-Si)$_3$phen/SiO$_2$ and PhA. (B) TGA curves of silica, APTES/SiO$_2$ and Eu(PhA-Si)$_3$phen/SiO$_2$.

The Fourier transform infrared (FT-IR) spectra of pure silica, intermediate product APTES/SiO$_2$, Eu(PhA-Si)$_3$phen/SiO$_2$ and PhA given in Fig. 1A could provide information of the functional groups in the materials. In the spectra, the vibration absorption peaks related to the asymmetric and symmetric stretching of the Si-O-Si bond in silica appear at wave numbers 1110 cm^{-1} and 808 cm^{-1} respectively. For, APTES/SiO$_2$, the bending vibrational peak at wave number 1642 cm^{-1} and the stretching vibrational absorption peak at 3450 cm^{-1} for the hydroxyls were weakened, attesting the successful reaction with APTES consuming the free hydroxyls in silica. In the spectrum of Eu(PhA-Si)$_3$phen/SiO$_2$, a vibrational absorption peak reflecting the carbonyls from PhA emerges at 1680 cm^{-1}, while the signal of the C–N stretching vibration at 1299 cm^{-1} verifies the amide formation.

Thermogravimetric (TGA) curves of the materials were given in Fig. 1B. The rapid weight loss of the first three solid materials before reaching 100 °C was caused by the thermal decomposition of the surface-adsorbed water. From 100 °C to 800 °C, the weight loss of SiO$_2$ slows down due to the difficulty in breaking the hydrogen bonds of silicon hydroxyl groups, which are involved in the form of bound water. Compared with SiO$_2$, the mass curve of APTES/SiO$_2$ declined faster. The thermogravimetric curve of the product Eu(PhA-Si)$_3$phen/SiO$_2$ after 100 °C was divided into two stages. The rapid decline from 250 °C to 350 °C and the slower decline after 400 °C reflected the dissociation of ligands and the decomposition of organic matter respectively. Based on the provided two charts, along with the transmission electron microscope (TEM) and mapping images depicted in Fig. S2 (Supporting information) [38], it was verified that the organometallic europium layer had been successfully introduced covering the surfaces of the silica particles.

A series of modified silicas (a-f) were then synthesized *via* similar methods, and their chemical structures were illustrated in Fig. 2. They were marked as Eu(PhA-Si)$_3$phen/SiO$_2$, Eu(NaA-Si)$_3$phen/SiO$_2$, Eu(BrA-Si)$_3$phen/SiO$_2$, Eu(DBM)$_2$(PhA-Si) phen/SiO$_2$, Eu(DBM)$_2$(NaA-Si)phen/SiO$_2$ and Eu(DBM)$_2$(BrA-Si) phen/SiO$_2$ respectively according to their chemical structures and the substituents. They were then employed in the experiments to examine the effects of phthalic anhydride (PhA), naphthalenedicarboxylic anhydride (NaA), 4-bromophthalic anhydride (BrA) and dibenzoyl methane (DBM) moieties onto the properties of the materials. 1,10-Phenanthroline(phen) was involved in all cases to enhance the stability of the organometallic europium moieties.

Fig. 3 provides the Fourier transform infrared (FT-IR) spectra, UV absorption spectra, fluorescence excitation and emission spectra of the materials for comparison. As shown in Fig. 3A, the FT-IR spectra of the materials are similar because they possess the same set of functional groups. For UV absorption spectra, the materials can be divided into two categories for study (Fig. 3B). First, for Eu(PhA-Si)$_3$phen/SiO$_2$, Eu(NaA-Si)$_3$phen/SiO$_2$ and Eu(BrA-Si)$_3$phen/SiO$_2$, the absorption peak around 200 nm corresponded to $n\rightarrow\sigma^*$ electron transition, while the peaks around 260–450 nm corresponded to π-π^* electron transition were generated by conjugation between the benzene ring and C=O functional group. The increased migration reduced the energy gap for molecular transitions, resulting in a redshift in curves b and c *vs.* a in the UV absorption spectra [39]. Electron-donating naphthalene could enhance the π electron density in the molecule, leading to the increase of the intensity of UV absorption. Moreover, due to the inductive effect, a redshift of the signal could occur. On the contrary, electron-withdrawing groups could cause blueshifts of the absorption peaks and the decrease in their intensities. In Fig. 3B, curves d-f were corresponding to the products with the addition of DBM. Due to the presence of a benzene ring bearing carbonyls (C=O) in the DBM moieties, the changes in absorption peaks corresponding to π-π^* electronic transitions were not obvious, but they generally followed the aforementioned rule as well [40,41].

The fluorescence excitation and emission curve data of six sets of experimental samples were then compared (Figs. 3C and D). Upon the addition of DBM, the fluorescence excitation ranges were widened from 260 nm to 300 nm to 260 nm to 420 nm. Due to its robust π-π^* conjugated structure, DBM enhances the absorption capacity of ultraviolet light. Upon ligand absorption of photon energy, the energy is transferred to the central rare-earth Eu^{3+} through the "antenna effect" electronic transition. Subsequently, Eu^{3+} transitions from the S_0 singlet state to the S_1 singlet state. It further undergoes intersystem crossing (ISC) to the triplet state T_1. When the electron returns from the excited triplet state to the ground state, characteristic fluorescence of rare-earth ions is emitted. DBM enhances the fluorescence excitation capability of rare-earth ligands, allowing fluorescence emission in wavelength ranges that were previously inaccessible [42-44]. Simultaneously, Eu(NaA-Si)$_3$phen/SiO$_2$ and Eu(DBM)$_2$(NaA-Si)phen/SiO$_2$ with larger π-π^* conjugated structures exhibit stronger fluorescence intensity. Conversely, Eu(BrA-Si)$_3$phen/SiO$_2$ and Eu(DBM)$_2$(BrA-Si)phen/SiO$_2$ with bromine-connected electron-withdrawing groups on the benzene ring show weaker UV absorption capacity and lower fluorescence intensity. To provide precise data support, we measured the Eu^{3+} content, fluorescence quantum efficiency, and fluorescence lifetime at 275 nm for all six samples. Detailed numerical values are listed in Table 1, indicating that ligands with larger π-π^* conjugated structures favor electron excitation, resulting in higher fluorescence quantum efficiency and lifetime. On the other hand, the presence of electron-withdrawing groups weakens fluorescence quantum efficiency and lifetime.

The newly developed fluorescently modified white carbon black exhibits greater fluorescence intensity and a broader fluorescence excitation range, facilitating its characterization in dispersed images within rubber. On the basis of the above experimental results, Eu(DBM)$_2$(NaA-Si)phen/SiO$_2$ was then chosen for analysis in the modified rubber filler experiment. Figs. 4A and B indicated that the silicon rubber filled with fluorescent-modified silica (b) emit-

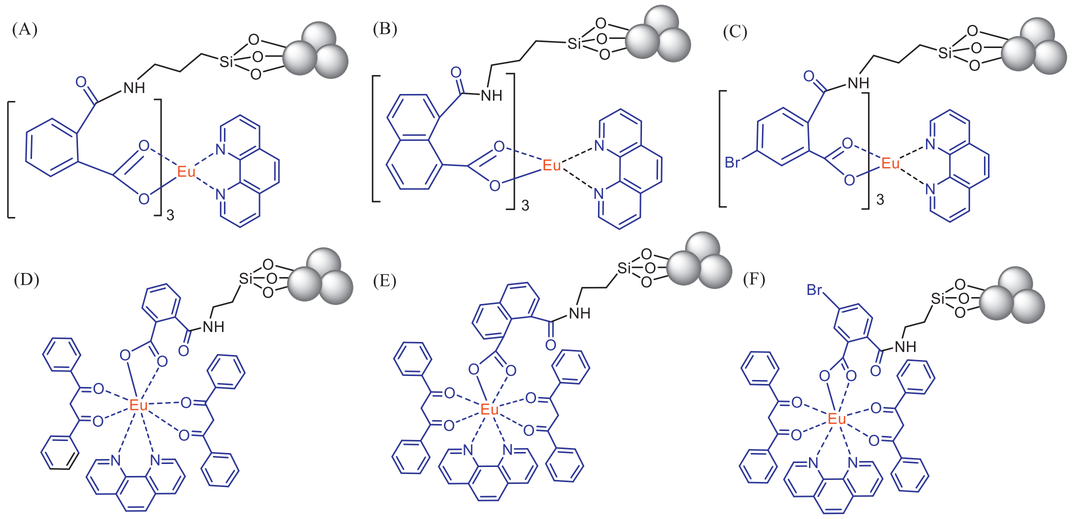

Fig. 2. Modified silicas: (A) Eu(PhA-Si)$_3$phen/SiO$_2$, (B) Eu(NaA-Si)$_3$phen/SiO$_2$, (C) Eu(BrA-Si)$_3$phen/SiO$_2$, (D) Eu(DBM)$_2$(PhA-Si)phen/SiO$_2$, and (E) Eu(DBM)$_2$(NaA-Si)phen/SiO$_2$, (F) Eu(DBM)$_2$(BrA-Si)phen/SiO$_2$.

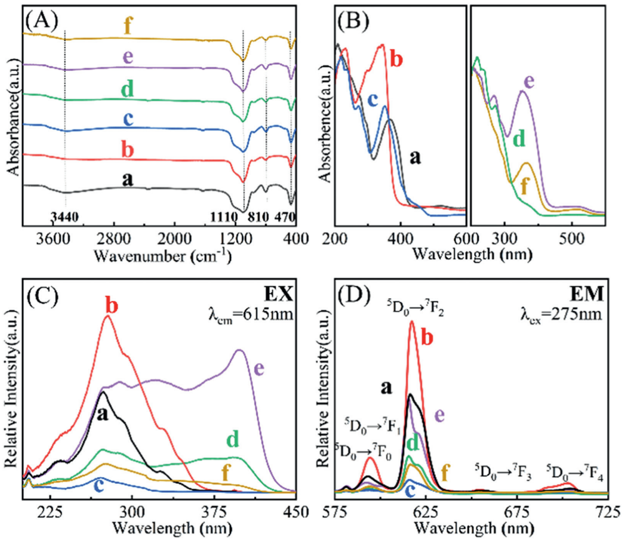

Fig. 3. (A) The FT-IR and (B) the ultraviolet absorption spectra of six different modified silica species. (C) The excition and (D) emission spectral characterizations of fluorescent modification silica. (a) Eu(PhA-Si)$_3$phen/SiO$_2$; (b) Eu(NaA-Si)$_3$phen/SiO$_2$; (c) Eu(BrA-Si)$_3$phen/SiO$_2$; (d) Eu(DBM)$_2$(PhA-Si) phen/SiO$_2$; (e) Eu(DBM)$_2$(NaA-Si)phen/SiO$_2$; (f) Eu(DBM)$_2$(BrA-Si)phen/SiO$_2$.

Table 1
The luminescence efficiencies and lifetime data for the hybrid materials.

Samples	Eu^{3+} [a]	QY [b]	FL [c]
Eu(PhA-Si)$_3$phen/SiO$_2$	6.7	39.22	503
Eu(NaA-Si)$_3$phen/SiO$_2$	7.0	47.71	762
Eu(BrA-Si)$_3$phen/SiO$_2$	12.7	20.62	510
Eu(DBM)$_2$(PhA-Si)phen/SiO$_2$	8.5	2.53	311
Eu(DBM)$_2$(NaA-Si)phen/SiO$_2$	5.1	12.00	539
Eu(DBM)$_2$(BrA-Si)phen/SiO$_2$	10.4	1.53	513

[a] Eu^{3+} quality ratio (%).
[b] Quantum yield (%).
[c] Fluorescence life (ms).

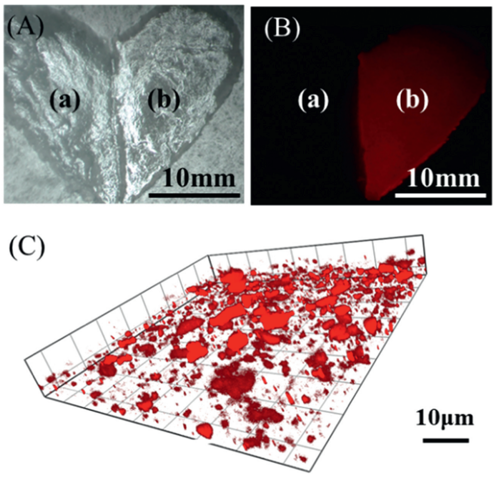

Fig. 4. Photographs of silicone rubber filled with pure SiO$_2$ (a) and Eu(DBM)$_2$(NaA-Si)phen/SiO$_2$ (b) under natural (A) and 365 nm ultraviolet light (B). (C) The 3D reconstruction images of the Eu(DBM)$_2$(NaA-Si)phen/SiO$_2$ (b) dispersed in rubber composite.

ted red light under UV light excitation, whereas the sample filled with pure silica did not emit any light. The 3D image shown in Fig. 4C was then established by accurately capturing more than 80 consecutive 2D confocal images at different focal planes through optical sectioning in the silica/rubber composite material (Fig. S3 in Supporting information). Characterization using TEM also yielded similar results to LSCM analysis (Fig. S4 in Supporting information). The filled silica is uniformly distributed in the rubber matrix, and there is no obvious difference in properties between rubbers filled with APTES/SiO$_2$ and Eu(DBM)$_2$(NaA-Si)phen/SiO$_2$ respectively (Fig. S5 and Table S1 in Supporting information). These results show that 3D fluorescence visualization can effectively exhibit the actual dispersion state of silica in the composite materials.

In conclusion, this paper presents the successful synthesis of a novel fluorescent coupling agent utilizing phen, DBM, and a silane coupling agent as rare earth Eu^{3+} ligands. The coupling agent was loaded onto the surface of silica and was employed as a fluorescent filler in rubber. The dispersion of silica in rubber is investigated through LSCM characterization. By altering the substituent of the silane coupling agent ligand, control over fluorescence intensity is achieved. Additionally, the introduction of a DBM ligand broadens the excitation wavelength range. This research introduces innovative perspectives for developing fluorescent fillers, facilitating quantitative analysis of the influence of micro dispersion state variations in fillers on the performance of rubber products. The novel fluorescent filler offers a more convenient and effective testing methodology, contributing to a comprehensive understanding of the structure-activity relationship between inorganic filled polymers and the performance of rubber products. This method affords more feasible solutions for visually studying the relationship between the submicroscopic structure and macroscopic properties of inorganic-filled polymers. It may also provide the technical basis for tracking the distribution of silica fillers in rubber complexes, endowing the automated quality monitoring in further industrial production line construction.

Declaration of competing interest

The authors declare that they have no known competing financial interests or personal relationships that could have appeared to influence the work reported in this paper.

CRediT authorship contribution statement

Junqing Wu: Investigation. **Yiyang Zhang:** Writing – original draft, Investigation. **Qingqing Hong:** Data curation. **Hui Yang:** Data curation. **Lifeng Zhang:** Supervision. **Ming Zhang:** Supervision. **Lei Yu:** Writing – review & editing, Supervision, Project administration, Conceptualization.

Acknowledgments

This project was financially supported by the Yangzhou Key Research and Development Program: Industry Foresight and Key Core Technology (No. YZ2023019), Cooperation Project of Yangzhou City with Yangzhou University (No. YZ2023209), Jiangsu Provincial Six Talent Peaks Project (No. XCL-090) and Priority Academic Program Development of Jiangsu Higher Education Institutions (PAPD). We also thank Yangzhou Bangjie New Materials Co., Ltd. for support. We thank Dr. Xu Zhang at Yangzhou University for assistances in experiments.

Supplementary materials

Supplementary material associated with this article can be found, in the online version, at doi:10.1016/j.cclet.2024.110165.

References

[1] B. Guo, F. Chen, Y. Lei, et al., Polym. J. 42 (2010) 319–326.
[2] E. Kontou, A. Christopoulos, P. Koralli, et al., J. Nanomater. 13 (2023) 1095.
[3] D. Liu, L. Song, H. Song, et al., Compos. Sci. Technol. 165 (2018) 373–379.
[4] A. McGlasson, K. Rishi, G. Beaucage, et al., Macromolecules 53 (2020) 2235–2248.
[5] X. Hao, K. Zhang, W. Ma, et al., Rare Metals 42 (2022) 70–75.
[6] Q. Ma, S. Wang, M. Wen, et al., Rare Metals 41 (2015) 3180–3185.
[7] X. Li, Q. Yang, H. Li, et al., Compos. B: Eng. 212 (2021) 108687.
[8] X. Li, Q. Yang, Y. Ye, et al., Compos. Part A: Appl. Sci. Manuf. 131 (2020) 105778.
[9] D. Liu, J. Chen, L. Song, et al., Polymer 120 (2017) 155–163.
[10] K. Nusser, T. Mosbauer, G.J. Schneider, et al., J. Non-Cryst. Solids 358 (2012) 557–563.
[11] Y. Shui, L. Huang, C. Wei, et al., Compos. Commun. 23 (2021) 100547.
[12] X. Kang, D. Liu, P. Zhang, et al., Chin. J. Polym. Sci. 38 (2020) 1006–1014.
[13] X. Li, C. Tian, H. Li, et al., Compos. Part A: Appl. Sci. Manuf. 152 (2022) 106722.
[14] Y. Sun, Z. Cheng, L. Zhang, et al., J. Appl. Polym. Sci. 137 (2020) 49526.
[15] D. Veigel, K. Rishi, U. Okoli, et al., Polymer 269 (2023) 125735.
[16] M. Nuriya, S. Fukushima, A. Momotake, et al., Nat. Commun. 7 (2016) 11557.
[17] Z. Li, P. Liang, T. Ren, et al., Angew. Chem. Int. Ed. 62 (2023) e202305742.
[18] K. Shin, J.W. Choi, G. Ko, et al., Nat. Commun. 8 (2017) 15807.
[19] P. Du, Y. Wei, Y. Liang, et al., Adv. Sci. 11 (2023) 2305308.
[20] D. Yue, M. Wang, F. Deng, et al., Chin. Chem. Lett. 29 (2018) 648–656.
[21] Y. Yang, Y. Liu, D. Tu, et al., Angew. Chem. Int. Ed. 61 (2022) e202116983.
[22] C. Tian, G. Chu, Y. Feng, et al., Compos. Sci. Technol. 170 (2019) 1–6.
[23] G.P. Baeza, A.C. Genix, C. Degrandcourt, et al., Macromolecules 46 (2012) 317–329.
[24] M. Ge, J. Wu, Q. Hong, et al., Anal. Methods 14 (2022) 3982–3988.
[25] K. Chen, M. Kang, A. Lu, et al., J. Mater. Sci. 54 (2018) 5149–5159.
[26] Z. Feng, J. Zhong, W. Guan, et al., Analyst 143 (2018) 2090–2095.
[27] W. Guan, S. Wang, C. Lu, et al., Nat. Commun. 7 (2016) 11811.
[28] L. Feng, W. Li, J. Bao, et al., Roy. Soc. Open Sci. 6 (2019) 190182.
[29] P. Dhankhar, R. Devi, S. Devi, et al., Rare Metals 41 (2019) 1342–1352.
[30] T. Ogawa, S. Ogoe, T.A. Asoh, et al., Compos. Sci. Technol. 198 (2020) 108277.
[31] Y. Xiong, S. Shen, M. Kang, et al., Polymer 208 (2020) 122904.
[32] U. Okoli, K. Rishi, G. Beaucage, et al., Polymer 264 (2023) 125407.
[33] K. Rishi, L. Pallerla, G. Beaucage, et al., J. Appl. Phys. 127 (2020) 174702.
[34] Y. Wang, M. Sun, H. Zhang, et al., Macromolecules 56 (2023) 934–946.
[35] S. Zeng, M. Kang, K. Chen, et al., Polym. Test. 90 (2020) 106749.
[36] J. Shi, Y. Wang, L. Huang, et al., Nanomaterials 9 (2019) 510.
[37] L. Wang, H. Liu, S. Huang, et al., Rare Metals 40 (2017) 728–735.
[38] J. An, C. Zhao, Z. He, et al., Rare Metals 41 (2022) 3351–3359.
[39] J.Y. Wu, J.D. Yang, J.P. Cheng, Eur. J. Inorg. Chem. 26 (2022) e202200556.
[40] J. Xu, F. Yan, X. Sun, et al., J. Photoch. Photobio. A 382 (2019) 111938.
[41] S.V. Eliseeva, J.C. Bunzli, Chem. Soc. Rev. 39 (2010) 189–227.
[42] L. Huang, J. Wang, H. Zhang, et al., J. Rare Earths 41 (2023) 60–66.
[43] S. Li, L. Zhou, H. Zhang, Light-Sci. Appl. 11 (2022) 177.
[44] Y. Wang, Q. Sun, L. Huang, et al., Nanomaterials 10 (2020) 1964.